

Colour corrections from atmospheric transmission with AuxTel for LSST.

Rodríguez Monroy, M.¹, Moniez, M.¹, Dagoret-Campagne, S.¹, Chevalier, J.¹, Neveu, J.¹, Ansari, R.¹, Perdereau, O.¹, and Campagne, J.E.¹

¹ Laboratoire de Physique des 2 infinis Irène Joliot-Curie (IJCLab), UMR9012 – CNRS, Bât. 100, 15 rue Georges Clémenceau, 91405 Orsay cedex

Abstract

Measuring colours is a crucial task for many of current and future cosmological surveys. Colour calibration is essential to obtain cosmological information from supernovae to photometric redshifts. In the coming years the Legacy Survey of Space and Time will start to carry out a massive survey which will provide data with statistical errors below the systematic uncertainty due to photometric calibration. Therefore, photometric calibration will be one of the main challenges in our way to obtain reliable cosmological measurements. One of the main sources of photometric uncertainty is associated with atmospheric transmission. We propose a method to derive colour corrections based on spectroscopic observations with the Auxiliary Telescope (AuxTel). In this method, we will measure the colour corrections to compensate for the effect of atmospheric transmission by measuring this transmission from spectro-photometric standard stars.

1 Introduction

When carrying out ground-based observations we wish to recover the photometric information (magnitudes, colours, etc) of the observed objects as if they were seen from top of atmosphere (TOA). Another possibility is to obtain this information for a standard atmosphere. In both cases, we need to apply some type of correction in order to obtain the desired photometry.

For a survey such as the Legacy Survey of Space and Time (Rubin-LSST) [1, 3] the colour information of the sources comes from observing their fluxes through broadband filters. In particular, the filters used by Rubin-LSST are *ugrizY*, which cover from 320 nm to 1080 nm. In the right hand side of Figure 1 the filter passbands are represented by the shaded regions with solid contours. The observed flux is the integrated product of the TOA spectral energy distribution (SED) of the source, $F_\nu(\lambda)$, and the filter passband, $S_{filter}^b(\lambda)$. However, the filters are not the only factor that determines the observed magnitude of an object. The optical throughput of the telescope affects the number of photoelectrons converted in the CCD. The throughput is the product of the filter passband with the efficiency of the different mirrors and of the disperser element in the case of spectroscopic observations, the quantum

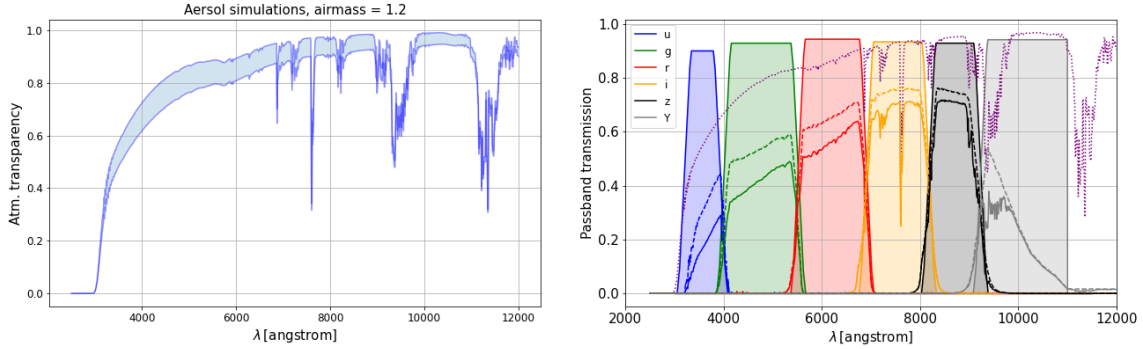


Figure 1: *Left*: simulated atmospheric transparencies obtained using *libRadtran* varying the amount of aerosols from 0.01 to 0.09 for airmass = 1.2, PWV = 3.0 mm, $O_3 = 300$ DU and no clouds. *Right*: filter passbands (shaded regions with solid contours), atmospheric transparency (dotted line), throughput of the telescope (dashed lines) and effective passbands (solid lines) of LSST telescope.

efficiency of the CCD and the transmission of the refractive elements (lenses, entrance window, etc). The product of all these wavelength dependent factors is $S_{inst}^b(\lambda)$.

Finally, the observed flux is also impacted by the atmospheric conditions. In particular, the concentrations of some of the components of the atmosphere, such as precipitable water vapour (PWV), aerosols or ozone, together with the airmass of observation have different effects on the atmospheric transparency, $S_{atm}(\lambda)$. For example, PWV has more impact on the redder part of the spectrum, inducing several telluric absorption lines, while aerosols are more important on the bluer wavelengths. The atmospheric transparency for different values of the aerosol concentration at an airmass of 1.2 is shown in the left hand side of Figure 1.

Then, the effective passband, $S_{obs}^b(\lambda)$, through which the light of a source goes through is the product of the throughput of the telescope and the atmospheric transparency given by the state of the atmosphere at the moment of observation. This way, the flux (in number of photons) observed through each filter is given by

$$F_{obs}^b \propto \int F_{\nu}(\lambda) \cdot S_{obs}^b(\lambda) \cdot \frac{d\lambda}{h\lambda}, \quad (1)$$

and from it is possible to compute the observed magnitudes, m_{obs}^b . Therefore, the atmosphere affects the magnitudes and thus the colours of the astronomical sources with respect to a reference case (e.g. TOA or a standard atmosphere). In the right hand side of Figure 1 we depict a certain atmospheric transparency (dotted line), the throughput of the LSST telescope (dashed lines) and the effective passbands (solid lines).

In this work, we present the basics of the colour correction method that we propose to employ for the photometry of LSST. This method makes use of the standard spectra observed by AuxTel to derive corrections by comparing with their corresponding TOA observations.

2 An auxiliary telescope for Rubin-LSST: AuxTel

The auxiliary telescope, AuxTel, is a 1.2m telescope equipped with a single CCD and located in Cerro Pachón, Chile, together with the Rubin-LSST's 8.4 m main telescope. Since 2021 AuxTel is taking data twice a month during 3-day long observing runs on average, making it the prototype instrument used for data management commissioning of Rubin-LSST.

AuxTel is equipped with a slitless spectrograph. Slitless spectroscopy has the advantage of not requiring a precise positioning of the source to make it coincident with the slit, thus making this technique much less time consuming. In addition, the absence of slit means that there is no loss light, allowing to perform spectro-photometric observations. On the other hand, this also implies that the subtraction of sky and stellar background must be performed more carefully and that the spectral resolution is limited by the seeing.

In order to obtain the spectra, a especially designed thin phase hologram [5] was installed in AuxTel. It was obtained by recording the interference pattern of two point sources at the zero-order position and at the desired first-order position (see Figure 2). Periodic gratings rely on the assumption that the incident beam is parallel, which is not the case, since the beam is convergent. Moreover, in the geometrical configuration of an imager, each wavelength is focused at different distances from the focal plane. These problems are overcome by the hologram, since it works with a convergent beam and each wavelength is correctly focused near the focal plane, allowing to reach the nominal resolution ($R > 200$ within [342,1100] nm) and to increase the signal-to-noise ratio. Figure 2 showcases the different focus positions as function of wavelength between a normal periodic grating and the hologram. The final mission of the spectrograph is to measure the atmospheric transmission so we can correct one by one the fluxes of the observed objects so we can recover their photometric information as if seen with standard atmospheric conditions.

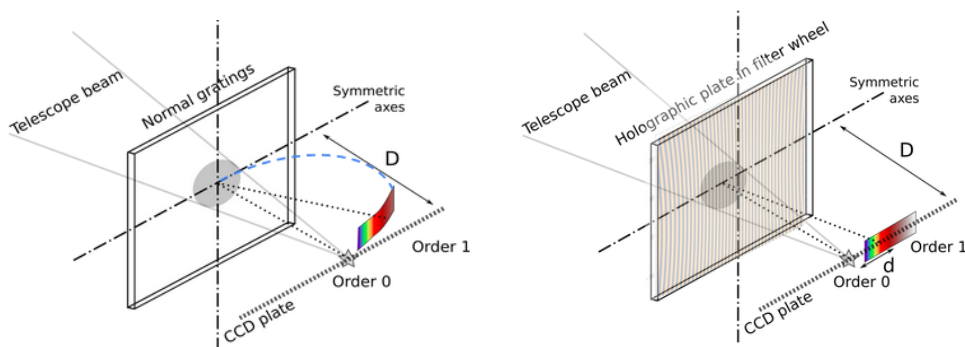


Figure 2: Difference between the focus position for each wavelength obtained with a periodic grating (left) and a holographic optical element (right) [5].

3 A colour correction method for Rubin-LSST

The final goal of the images obtained with a survey such as Rubin-LSST is to infer cosmological information from them. In this regard, there are different ways of working with the images. For example, galaxy clustering and weak-lensing analyses make use of coadded images, obtained by stacking the individual images to reach higher depths. On the other hand, transient object analyses, such as the study of the lightcurves of SNe Ia, use individual images. The differences between cosmological probes imply different photometric calibration requirements. The official Rubin-LSST precision goal is 10 mmag, while for SNe Ia the desirable goal is 1 mmag.

From the point of view of photometric calibration, there are two main sources of systematic uncertainty: the instrumental signature, caused by a plethora of effects (e.g. vignetting, filter transmission variations over time and position, electronic gains, non-linearities, PSF, etc), and the atmospheric absorption. Furthermore, both elements are wavelength dependent. As introduced in Section 1, we can express the effective passband as

$$S_{obs}^b(x, y, alt, az, t, \lambda) = S_{inst}^b(x, y, t, \lambda) \cdot S_{atm}(alt, az, t, \lambda), \quad (2)$$

where the subscript b represents each photometric filter, x, y correspond to the CCD coordinates, t is the time of observation, alt, az are the altitude and azimuth coordinates and λ is the wavelength. In order to correct the impact of both effects on photometry, we need to apply corrections to compensate them within the precision requirements.

The current proposal to obtain such photometric corrections for Rubin-LSST is to use the Forward Global Calibration Method (FGCM) [2]. It assumes that passbands vary over time, so it defines a standard passband that corresponds to standard atmospheric conditions. Then, it computes the correction as the difference between the observed and standard magnitudes.

Here we present the basics of a method proposed as an alternative to FGCM. The main idea behind it is to infer the atmospheric transparency and the amount of different atmospheric components in real time using the spectrograph placed in AuxTel. For this task, we use a set of standard spectra that have been observed from space, such as HST or Gaia standards. The main steps of the method are the following:

- We generate a set of atmospheric simulations using the *libRadtran* software [4] by varying one of the atmospheric parameters while keeping the others fixed. These parameters are PWV, aerosols and ozone. We can also vary the airmass and the cloudiness. Then, for each simulated atmospheric transparency we generate the effective passband multiplying by the telescope's throughput.
- We pass each standard SED through each of the simulated passbands (see Equation 1), obtaining the observed fluxes at different atmospheric conditions. An example of this is shown in the left panel of Figure 3.
- For each simulated flux we compute the observed colours: $u - g$, $g - r$, $r - i$, $i - z$ and $z - Y$. Then, we define Δc_i as the difference of a given colour, c_i , with respect to the colour expected with a standard atmosphere that we fix beforehand. Then, we obtain

the variation of colour, Δc_i , as a function of the atmospheric parameters, enabling us to determine the colour correction that needs to be applied to each object in order to recover the standard photometry. This is shown in the right panel of Figure 3. By doing this, we populate an N -dimensional space with the N observed colours of each SED and the corresponding correction.

- Finally, when observing with LSST we can identify to which hyper-volume element belongs each observed object based on its colours, so we can apply the corresponding colour correction to it.

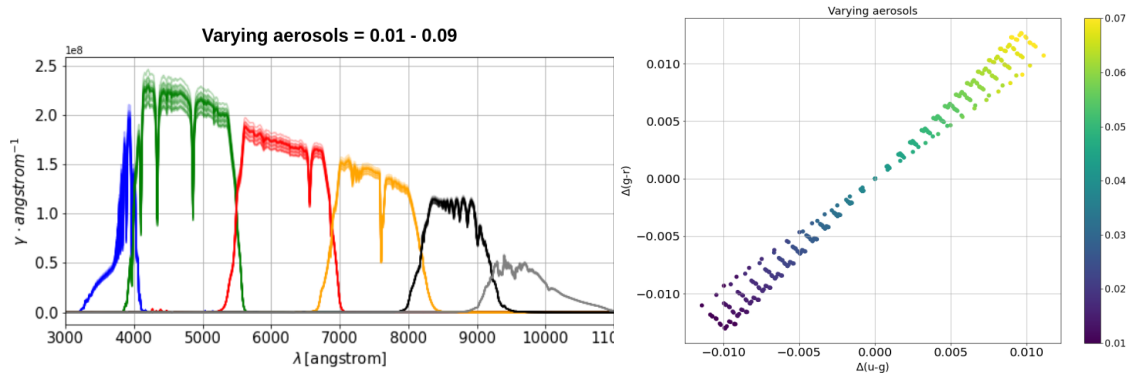


Figure 3: *Left*: standard star flux observed through the different simulated passbands, which take into account the different atmospheric transmissions. *Right*: colour evolution of different standards as a function of simulated values of aerosols.

Since LSST uses broadband filters, the shape of the SED plays an important role. For example, high aerosols concentrations have more impact on hotter (i.e. bluer) stars, making them to appear redder. On the other hand, high PWV values have more impact on the redder wavelengths, so colder (i.e. redder) stars appear bluer. For this reason, we consider the spectral type as a variable to populate the N -dimensional parameter space from which we determine the colour corrections.

We have tested our sensitivity to various observing conditions by measuring the equivalent width (EW) of stellar and telluric lines on the spectra of reference stars. While the EW of the stellar lines only depend on stellar and interstellar physics, the EW of the telluric lines depends on the atmosphere. In particular, we evaluate its dependence with the airmass, which traces the O_2 column density. Our preliminary results, presented in Figure 4, show that we are sensitive to variations on the amount of O_2 and H_2O .

4 Summary and prospects

In this contribution we present the basics of a new method proposed to obtain colour corrections for Rubin-LSST using of the spectra obtained with the holographic optical element installed in AuxTel. Our preliminary results with simulations show that we need $\sim 10\%$

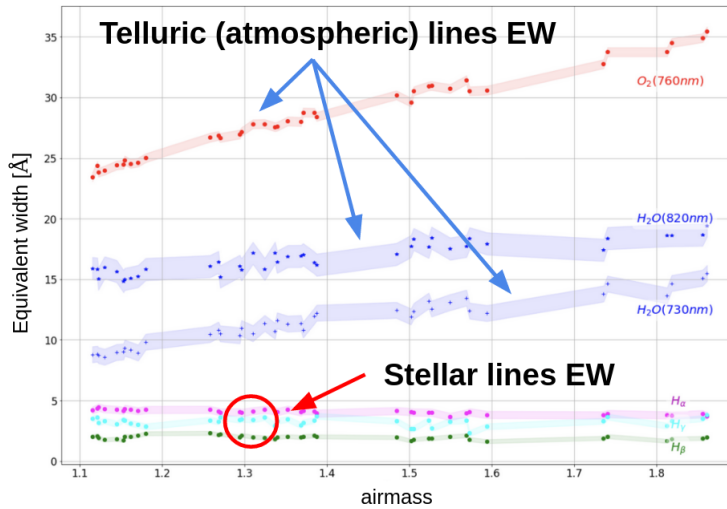


Figure 4: Equivalent width of stellar and telluric absorption lines. The former does not depend on the airmass and other atmospheric parameters, while the telluric ones show a clear dependence, proving our sensitivity to variations on the atmospheric parameters.

precision on the determination of atmospheric parameters to achieve 5 mmag precision in the photometric corrections. This is especially important for SNe Ia cosmological analyses carried out within Rubin-LSST. To apply this method, we use spectra of objects observed from space to compare them with the results obtained after passing through the atmosphere. This allows us to compute the correction on the colours to recover a reference photometry, such as that of a standard atmosphere for the site of observations.

Since AuxTel is slower than LSST, it will be usually pointing to a different position on the sky from LSST. Thus, we will use the atmospheric parameters derived by AuxTel to model the atmosphere in the direction that LSST is pointing to and then we will apply our method to obtain the corresponding correction. If both telescopes are observing the same position of the sky at the same time, we will directly obtain the atmospheric transparency by evaluating the ratio of the TOA and observed spectra of the standards on the field of view and we will correct the photometry consequently. Finally, the estimations of atmospheric parameters provided by AuxTel can serve as a prior to FGCM, allowing to use both in combination.

References

- [1] Abell, P.A. et al. [LSST Science Collaboration], 2009, arXiv, arXiv:0912.0201
- [2] Burke, D. L. et al., 2018, AJ, 155, 41
- [3] Ivezić, Z. et al., 2019, ApJ, 873, 111
- [4] Mayer, B. & Kylling, A., Atmos. Chem. Phys., 5: 1855-1877, 2005
- [5] Moniez, M., Neveu, J. Dagoret-Campagne, S., Gentet, Y., Le Guillou, L., 2021, MNRAS, 506, 5589